JACS
JOURNAL OF THE AMERICAN CHEMICAL SOCIETY
pubs.acs.org/JACS
Article

# Microenvironment-Sensitive Fluorescent Nucleotide Probes from Benzofuran, Benzothiophene, and Selenophene as Substrates for DNA Polymerases

Pulak Ghosh, Heike M. Kropp, Karin Betz, Samra Ludmann, Kay Diederichs, Andreas Marx,* and Seergazhi G. Srivatsan*

Cite This: J. Am. Chem. Soc. 2022, 144, 10556−10569
Read Online



**ABSTRACT:** DNA polymerases can process a wide variety of structurally diverse nucleotide substrates, but the molecular basis by which the analogs are processed is not completely understood. Here, we demonstrate the utility of environment-sensitive heterocycle-modified fluorescent nucleotide substrates in probing the incorporation mechanism of DNA polymerases in real time and at the atomic level. The nucleotide analogs containing a selenophene, benzofuran, or benzothiophene moiety at the C5 position of 2′-deoxyuridine are incorporated into oligonucleotides (ONs) with varying efficiency, which depends on the size of the heterocycle modification and the DNA polymerase sequence family used. KlenTaq (A family DNA polymerase) is sensitive to the size of the modification as it incorporates only one heterobicycle-modified nucleotide into the growing polymer, whereas it efficiently incorporates the selenophene-modified nucleotide analog at multiple positions. Notably, in the single nucleotide incorporation assay, irrespective of the heterocycle size, it exclusively adds a single nucleotide at the 3′-end of a primer, which enabled devising a simple two-step site-specific ON labeling technique. KOD and Vent(exo-) DNA polymerases, belonging to the B family, tolerate all the three modified nucleotides and produce ONs with multiple labels. Importantly, the benzofuran-modified nucleotide (BFdUTP) serves as an excellent reporter by providing real-time fluorescence readouts to monitor enzyme activity and estimate the binding events in the catalytic cycle. Further, a direct comparison of the incorporation profiles, fluorescence data, and crystal structure of a ternary complex of KlenTaq DNA polymerase with BFdUTP poised for catalysis provides a detailed understanding of the mechanism of incorporation of heterocycle-modified nucleotides.

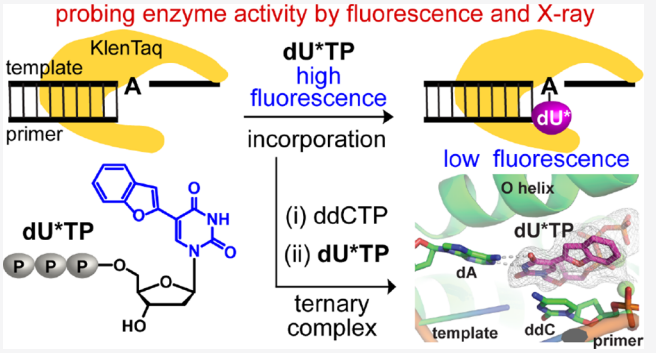




## INTRODUCTION

Enzymatic functionalization of nucleic acids with biophysical tools and probes is used in many biotechnological applications as well as in fundamental research of nucleic acid structure and function.[1−5] This process greatly relies on the ability of native and engineered DNA and RNA polymerases and transferases to incorporate functionalized nucleotides into oligonucleotides (ONs).[6−17] Though unpredictable, base-modified nucleotide analogs, which do not affect the Watson−Crick base paring, are reasonably well-tolerated by these enzymes.[18,19] For example, nucleotide analogs bearing fluorophores, redox-, NMR-, and EPR-active labels[20−27] and nucleotides containing handles for postsynthetic modification are widely employed.[28−32] A notable number of analogs are also metabolically incorporated by endogenous enzymes, which has further enabled the profiling and visualization of endogenous nucleic acids in living cells.[33−38] However, the mechanism by which polymerases accept unnatural nucleotides as substrates and incorporate them into the nascent nucleic acid chains is not yet fully understood, so prediction of substrate tolerance is often not possible. Nevertheless, "platforms" have been established by combining biochemical techniques and X-ray crystallography to gain functional and structural insights into the mechanism of acceptance and incorporation of certain modified nucleotides by DNA polymerases.[18,39] Successful co-crystallization of a truncated version of *Thermus aquaticus* DNA polymerase, KlenTaq, in complex with a primer•template duplex and 2′-deoxynucleoside triphosphate (dNTP) surrogates provided structural basis for the processivity of the DNA polymerase.[18] Polar flexible modifications (e.g., amino-

Received: March 31, 2022
Published: June 6, 2022




https://doi.org/10.1021/jacs.2c03454
J. Am. Chem. Soc. 2022, 144, 10556−10569

pentynyl) and a nonpolar aromatic group (e.g., ethynylbenzene) attached to C5 of pyrimidines or C7 of 7-deazapurines *via* an alkyne bond tend to stabilize substrate−enzyme interaction and show good incorporation efficiency.[40,41] In contrast, a rigid and nonpolar spin label connected to a nucleotide distorts the enzyme conformation and thus its efficiency of incorporation.[42] Though these studies are indicative, a comprehensive understanding of the chemical space that can be handled by nucleic acid processing enzymes is very important. In this context, as the next important step, we sought to investigate the ability of DNA polymerases to process heterocycle-modified environment-sensitive fluorescent nucleotide probes because they represent an important class of biophysical tool boxes in the analysis of nucleic acid.[43−46]

Environment-sensitive fluorescent nucleoside analogs derived by conjugating or fusing heterocyclic groups to pyrimidine and purine bases are highly valuable in probing conformations, dynamics, and recognition properties of nucleic acids.[47−52] A notable number of such responsive analogs are amicable to enzymatic incorporation by polymerases and are useful in studying nucleic acid lesions, nucleic acid−drug/protein binding, and conformations of therapeutically relevant nucleic acid motifs including bacterial ribosomal decoding site and tetraplexes.[53−57] While the incorporation efficiency by different polymerases varies, which is typically determined by gel electrophoresis, the structural basis by which the fluorescent nucleotide analogs are accepted and processed by different families of DNA polymerases has not been well studied. Here, our idea is to devise a platform by harnessing the inherent responsiveness of the fluorescent nucleotide substrates and X-ray crystallography technique to probe the mechanism of enzymatic incorporation. For this purpose, we chose three nucleobase modified 2′-deoxyuridine-5′-triphosphate substrates, each containing a benzofuran, benzothiophene, or selenophene moiety, as the test system (Figure 1). Notably, these base-modified fluorescent nucleoside analogs are highly conformation-sensitive and show great promise in probing the structure and ligand binding of therapeutic nucleic acid motifs.[53,57−59] Characterizing the enzymatic incorporation of this set of fluorescent nucleotides has two advantages apart from understanding the role of expanded chemical space compared to the existing structural information−(i) the substrates themselves could serve as probes providing real-time fluorescence readout to study the events in the catalytic cycle under equilibrium conditions and (ii) the incorporation efficiency and binding data determined by biochemical and fluorescence assays could be directly correlated with the structure obtained by X-ray crystallography.

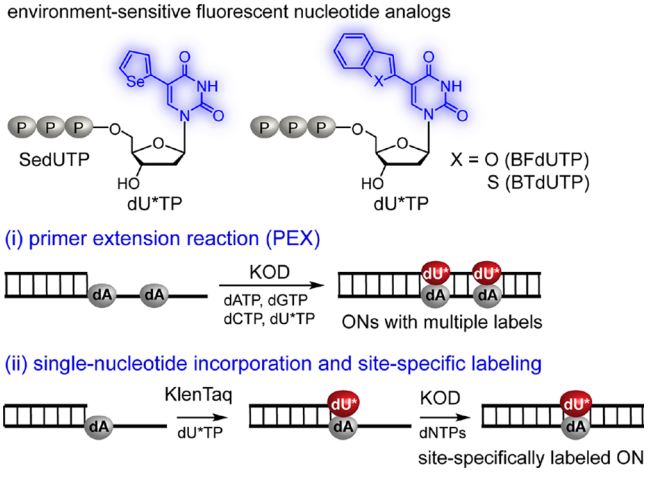


**Figure 1.** C5 heterocycle-conjugated fluorescent dU*TP analogs. The analogs are suitable for enzymatic functionalization of ONs by DNA polymerases. Depending on the enzyme choice and size of the heterocycle modification, ONs with (i) multiple labels and (ii) site-specific labels can be synthesized.

Here, we report the synthesis and incorporation of microenvironment-sensitive fluorescent nucleotide analogs, which are derived by conjugating benzofuran, benzothiophene, and selenophene at the C5 position of 2′-deoxyuridine (Figure 1). The nucleotide analogs are incorporated into ONs by KlenTaq (belonging to the sequence family A DNA polymerases), KOD, and Vent(exo-) DNA polymerases (both belonging to the B family) with varying efficiencies depending on the size of the heterocycle modification. KOD and Vent(exo-) DNA polymerases tolerate these modifications well and hence are suited for synthesizing ONs with multiple labels. In contrast, KlenTaq exclusively adds a single nucleotide analog at the 3′-end, thereby enabling the development of a simple two-step site-specific labeling procedure by PEX (Figure 1). Further, we describe the mechanism of incorporation of heterocycle-modified nucleotides by different families of DNA polymerases, which was obtained by comparing the incorporation profile, complex formation monitored using the responsiveness of the nucleotide analog, and X-ray structures of ternary complexes (enzyme−duplex−nucleotide) containing native and modified nucleotides.

## RESULTS AND DISCUSSION

**Design and Synthesis of Fluorescent Nucleotide Analogs.** We became interested in the C5 heterocycle-modified pyrimidine nucleotides **5**−**7** and their incorporation into ONs by DNA polymerases for the following reasons (Scheme 1). Conjugation of heterocycles at the C5 position of pyrimidines via a rotatable bond (molecular rotor element)[60,61] generates conformation-sensitive fluorescent probes (Figure 1).[25,43,46,62,63] Moreover, modifications at the C5 position of pyrimidines that can be accommodated in the major groove of duplexes show good substrate properties in DNA polymerization reactions.[3,18,64−72] Benzofuran (**2**), benzothiophene (**3**), and selenophene (**4**)-conjugated 2′-deoxyuridine analogs were synthesized by reacting 5-iodo-2′-deoxyuridine **1** with respective stanylated heterocycles under Stille cross-coupling reaction conditions using a palladium catalyst, $Pd(PPh_3)_2Cl_2$ (Scheme 1). These nucleoside analogs possess moderate quantum yields, and their photophysical properties are highly sensitive to microenvironment polarity and viscosity changes.[57,59,73] In particular, **2** and **4** incorporated into the human telomeric repeat ON by solid-phase synthesis enabled the conformational analysis and estimate the ligand binding ability of different G-quadruplex topologies by fluorescence and X-ray crystallography techniques.[57,59] To probe the DNA polymerase activity, the analogs were further converted to nucleoside 5′-triphosphates **5**, **6**, and **7** in a single-pot two-stage reaction using $POCl_3$ and *bis*-tributylammonium pyrophosphate (Scheme 1). The fluorescence profile, quantum yield, and lifetime of triphosphates **5**−**7** were similar to respective nucleoside analogs (Figure S1 and Table S1).

**DNA Polymerases Show Varying Incorporation Efficiency.** The potential of the three modified nucleotides


https://doi.org/10.1021/jacs.2c03454
J. Am. Chem. Soc. 2022, 144, 10556−10569

**Scheme 1. Synthesis of BFdUTP 5, BTdUTP 6, and SedUTP 7**[a]

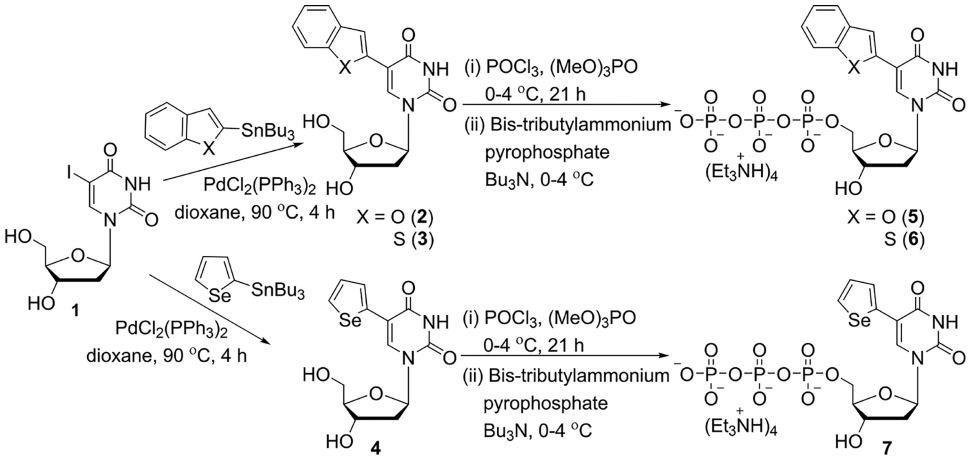


[a]See the SI for experimental details.

**Table 1. ON Sequences Used in PEX, Single Nucleotide Incorporation and Crystallization Studies, and Fluorescence assays**[a]

| ONs | Sequence |
|---|---|
| **P1** | 5′ FAM-GTG GTG CGA AAT TTC TGA CAG ACA 3′ |
| **T1** | 3′ CAC CAC GCT TTA AAG ACT GTC TGT **A**CT GTC TGC GTG 5′ |
| **T2** | 3′ CAC CAC GCT TTA AAG ACT GTC TGT GCT GTC T**A**C GTG 5′ |
| **T3** | 3′ CAC CAC GCT TTA AAG ACT GTC TGT GCT GT**A** T**A**C GTG 5′ |
| **T4** | 3′ CAC CAC GCT TTA AAG ACT GTC TGT GCT GTC T**AA** GTG 5′ |
| **T5** | 3′ CAC CAC GCT TTA AAG ACT GTC TGT GCT GT**A** T**AA** GTG 5′ |
| **P2** | 5′ FAM-GGA GCT CAG CCT TCA CTG C 3′ |
| **P3** | 5′ GGA GCT CAG CCT TCA CTG C 3′ |
| **T6** | 3′ CCT CGA GTC GGA AGT GAC G **A**CG ATT TGA TAT AAC GAT CGC GTG 5′ |
| **P2*** | 5′ FAM-GGA GCT CAG CCT TCA CTG C-**BFdU** 3′ |
| **P3*** | 5′ GGA GCT CAG CCT TCA CTG C-**BFdU** 3′ |
| **T7** | 3′ CCT CGA GTC GGA AGT GAC G ATG TCG CTC CGC GTC 5′ |
| **P4** | 5′ GAC CAC GGC CA 3′ |
| **T8** | 3′ CTG GTG CCG GT**G** **A**CAA 5′ |
| **P5** | 5′ GGA GCT CAG CCT TCA CTG ddC 3′ |

[a]ON primer **P1** and templates **T1**−**T5** were used in PEX. ONs **P2**/**P3** and **T6** were used in single-nucleotide incorporation reactions. **P2*** and **P3*** are 3′-BFdU-labeled primers **P2** and **P3**, respectively. **P3*** was used in fluorescence assays. Template **T7** was used in binding studies by fluorescence and EMSA. 2′-Deoxyadenosines colored in red in template strands guide the incorporation of modified nucleotides analogs in the PEX and single nucleotide incorporation assays. ONs **P4** and **T8** were used in crystallization trails. In **T8**, 2′-deoxyguanosine colored in blue is used for terminating the extension by using ddCTP in crystallization trails.

to serve as a thymidine analog for DNA polymerases was tested in primer extension reactions (PEX) in the presence of commonly used A and B family DNA polymerases. A series of templates (**T1**−**T5**) were designed to guide the incorporation of the modified nucleotides at the PEX start site, distal from the start site, and at multiple positions (Table 1). A 5′-FAM-labeled primer **P1** was hybridized with the respective templates, and the reactions were performed in the presence of dATP, dGTP, dCTP, and dTTP/modified dU*TPs (**5**−**7**, Figure 2A). Reaction products were resolved by polyacrylamide gel electrophoresis (PAGE) under denaturing conditions and visualized using a gel fluorescence scanner. Reactions were first performed with **T1** and **T2** that would guide the incorporation of a single modified nucleotide analog at the start site and away from the start site, respectively. Regardless of the size of modification, KlenTaq belonging to the A family efficiently incorporated the mononucleotides of **5**−**7** to produce full-length PEX products (Figure 2B, lanes 5−7 and lanes 10−12). The incorporation efficiency was as good as the reaction performed in the presence of natural dTTP (compare with lanes 4 and 9). When control reactions were performed in the absence of dTTP/modified dU*TPs but in the presence of other dNTPs, the enzyme did not produce full-length products (lanes 3 and 8). These results indicate that indeed the modified dU*TPs are incorporated specifically opposite to the templating dA and the full-length products are not formed due to misincorporation. However, with templates **T3** and **T4** that would introduce two modifications at alternate and consecutive sites, the incorporation efficiency was found to depend on the size of modification. While mononucleotides of benzofuran- and benzothiophene-modified dUTPs (**5** and **6**) were barely incorporated, selenophene-modified dUTP **7** was processed with an apparent efficiency as the natural nucleotide (Figure 2C, lanes 4−7 and lanes 9−12). When the stringency of incorporation was further increased by using **T5** (three modifications in close positions), KlenTaq did not produce full-length products with **5** and **6** (Figure S2, lanes 5 and 6). However, the enzyme tolerated the smaller selenophene modification and produced the triply-modified ON product in very good yields (Figure S2, lane 7).

Next, the B family DNA polymerases were investigated. BFdUTP **5**, BTdUTP **6**, and SedUTP **7** were processed


https://doi.org/10.1021/jacs.2c03454
J. Am. Chem. Soc. 2022, 144, 10556−10569

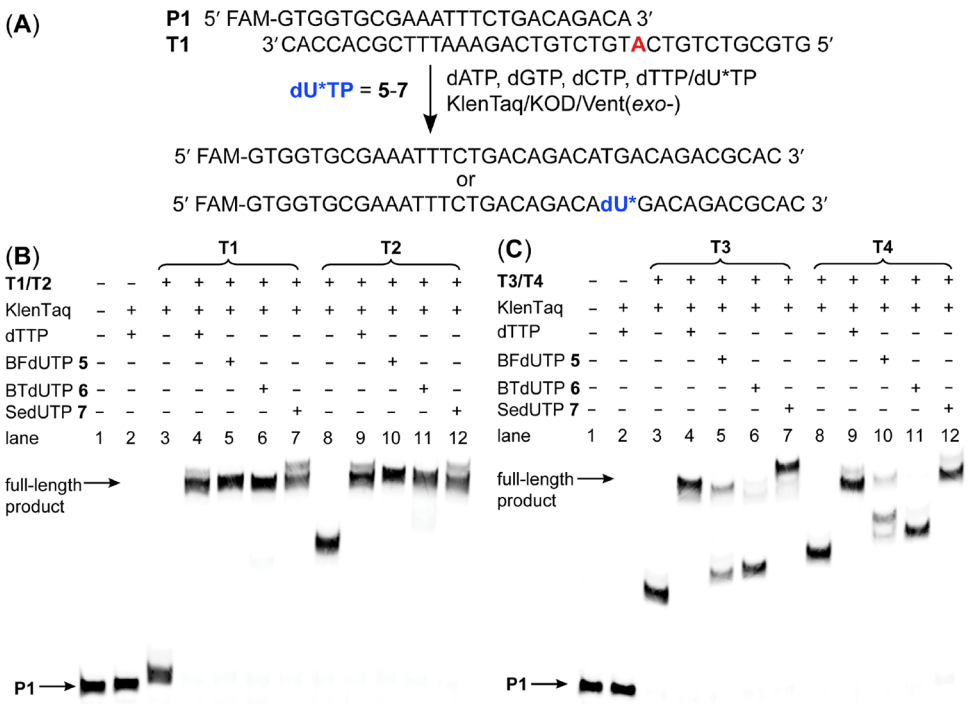


**Figure 2.** (A) PEX setup used to incorporate the mononucleotide analogs of **5**−**7** using different DNA polymerases. Reaction setup using **T1** is given as an example. (B,C) Incorporation of mononucleotides of BFdUTP **5**, BTdUTP **6**, and SedUTP **7** by KlenTaq using primer **P1** and templates **T1**−**T4**. All reactions were conducted in the presence of dATP, dGTP, and dCTP. For reactions with **T5**, see Figure S2.

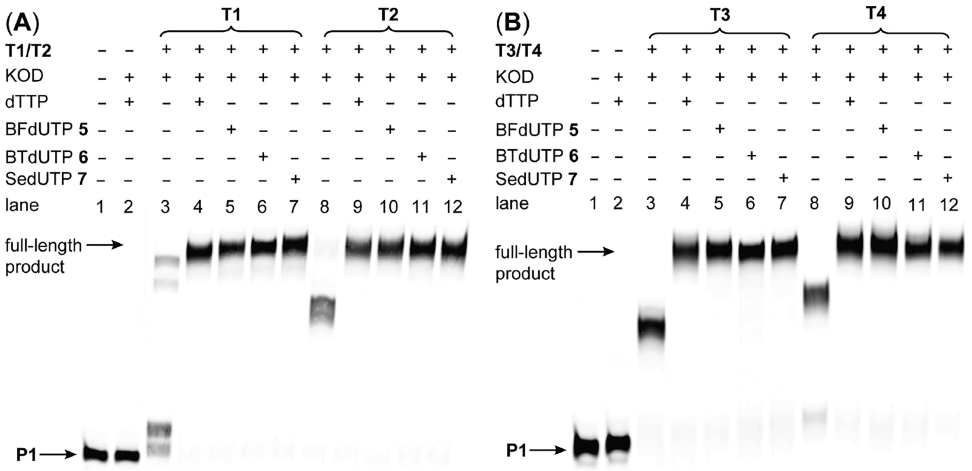


**Figure 3.** Incorporation of mononucleotides of BFdUTP **5**, BTdUTP **6**, and SedUTP **7** by KOD DNA polymerase using primer **P1** and templates **T1**−**T4**. All reactions were conducted in the presence of dATP, dGTP, and dCTP. For reactions with **T5**, see Figure S2.

proficiently by KOD using templates **T1**−**T5**, generating the full-length products with yields similar to the products formed in the presence of native dNTPs (Figure 3 and Figure S2, lanes 10−13). Similarly, all the heterocycle-modified nucleotides (**5**−**7**) served as good substrates for Vent(exo-), belonging to the same family of DNA polymerases (Figure S3). In the presence of **T1**−**T5**, the enzyme produced fully extended primers containing one or more modifications near and away from the start site. Taken together, KOD and Vent(exo-) DNA polymerases generate full-length products with all the tested templates and nucleotides while KlenTaq has difficulties with more demanding templates (two templating adenosines in a row or one nucleotide apart) and can generate multiple labeled full-length products only with the smaller modified SedUTP.

**Single Nucleotide Incorporation and Site-Specific Labeling.** Site-specific labeling of ONs with only one functional group is difficult using templates that contain the respective templating nucleotide at several positions (e.g., **T6**). Therefore, we chose to develop a two-step protocol by first incorporating one modified nucleotide and after a reaction clean-up (to remove the unreacted modified triphosphate) adding the four natural nucleotides to get the full-length product by PEX (Figure 4A). A prerequisite for the used enzyme should be that it faithfully incorporates only one modified nucleotide at the 3′-end of the primer in a template-dependent manner while it also fully elongates the modified primer with natural substrates or the singly modified primer should be compatible for enzymatic ligation.[74−79] In order to establish such a method, we tested single nucleotide


https://doi.org/10.1021/jacs.2c03454
J. Am. Chem. Soc. 2022, 144, 10556−10569

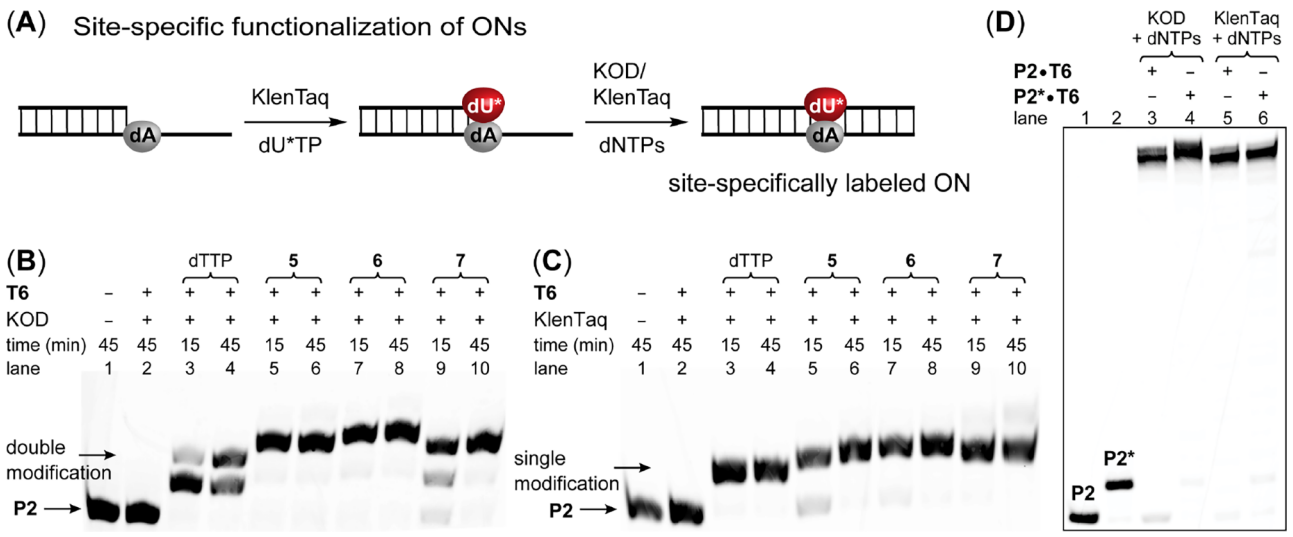


**Figure 4.** (A) Schematic diagram illustrating the site-specific functionalization approach. dU*TP represents a modified nucleotide analog probe. (B) In the presence of dTTP or modified nucleotides (**5**−**7**), KOD DNA polymerase added two consecutive nucleotides to the primer **P2**. (C) KlenTaq DNA polymerase produced only singly-modified ONs. (D) 3′-BFdU-labeled primer **P2*** was efficiently extended by KOD and KlenTaq DNA polymerase to give the full-length site-specifically functionalized ON product **P2****. See Table 1 and Table S3 for ON sequences.

incorporation properties of KOD and KlenTaq in the presence of modified nucleotides. A 5′-FAM-labeled primer **P2** was hybridized with a template DNA ON **T6** containing a dA nucleotide that would guide the incorporation of a modified mononucleotide at the 3′-end of the primer. Reactions in the presence of KOD DNA polymerase resulted in largely doubly modified ON products due to one correct incorporation of dU* opposite dA and one misincorporation of dU* opposite dC (Figure 4B). Attempts to obtain a singly modified primer with KOD DNA polymerase by varying the concentration of the enzyme and dU*TP were not successful (data not shown). Rewardingly, KlenTaq DNA polymerase incorporated all the three modified nucleotides with approximately same apparent efficiency as dTTP, yielding exclusively singly-modified primer ON products (Figure 4C). To unambiguously confirm the formation of singly-labeled products, large-scale reactions were performed and the identity of the isolated products was confirmed by mass analysis (Table S2 and Figure S4). Typically, reactions performed in a 1.25 nmol scale and purified by PAGE gave 60−70% of the labeled products.

Encouraged by these results, we devised a two-step template-dependent site-specific labeling technique by combining the stringent and flexible processivity of KlenTaq and KOD DNA polymerases, respectively. In the first step, the **P2•T6** duplex was reacted with BFdUTP in the presence of KlenTaq, which resulted in the quantitative incorporation of a single BFdU label at the 3′-end to produce ON **P2*** (Figure 4D, lane 2). The reaction mixture was heated, and the modified primer•-template duplex was precipitated using ethanol and washed well. This step was performed to inactivate the enzyme and remove the unreacted modified nucleotide. The precipitated **P2*•T6** duplex was annealed in the reaction buffer in the same tube and was subjected to PEX in the presence of dNTPs and KOD. The reaction resulted in almost quantitative production of the full-length site-specific labeled ON product **P2**** (Figure 4D lane 4, Table S3). A control PEX reaction performed in the presence of the **P2•T6** duplex and dNTPs confirmed the formation of the full-length product formed in the presence of the modified primer•template duplex (compare lanes 3 and 4, products move with a similar mobility). The identity of product **P2**** was further ascertained by mass analysis (Figure S4E and Table S2). The site-specific labeling could also be achieved using KlenTaq in the second step as it efficiently processed the modified primer•template duplex to give the full-length product in the presence of all four natural nucleotides (Figure 4D, lane 6). If required, the template can be specifically digested using lambda exonuclease giving access to the labeled single-stranded ON.[80] Collectively, these results indicate that the size of the heterocycle modification does not matter in the single nucleotide incorporation step using KlenTaq as it selectively incorporates all three modified dU*MPs opposite one templating adenosine. Furthermore, it does not show misincorporation of a second nucleotide as it is the case with KOD DNA polymerase rendering it superior for the first step in the site-specific labeling approach while for the elongation KlenTaq as well as KOD DNA polymerases can be used. This method could allow the site-specific installation of a variety of nucleoside probes, which can be used for nucleic acid conformation and function analysis.[5,43−45,56]

**Responsive Fluorescent BFdU Provides Insights on the Enzyme−Primer•Template Duplex Complex Formation.** To study the efficacy of the nucleotide substrates to serve as probes to monitor the binding processes involved in the polymerization reaction, we performed fluorescence assays. For this purpose, BFdU was chosen as it has been found to be more emissive and highly sensitive to its local environment.[53,59] The enzyme first forms a complex with the primer•template duplex and then the cognate nucleotide binds to the active site to form the ternary complex. We first studied the effect of modification on the binary complex (enzyme−primer•template duplex) formation by incubating unmodified **P2•T7** and 3′-BFdU-modified **P2*•T7** duplexes with increasing concentrations of KlenTaq. Electrophoretic mobility shift assay (EMSA) performed under non-denaturing conditions clearly revealed the formation of binary complexes, wherein BFdU-modified ($K_d$ = 0.24 ± 0.04 $\mu$M) and native ($K_d$ = 0.23 ± 0.03 $\mu$M) duplexes exhibited similar binding


https://doi.org/10.1021/jacs.2c03454
J. Am. Chem. Soc. 2022, 144, 10556−10569

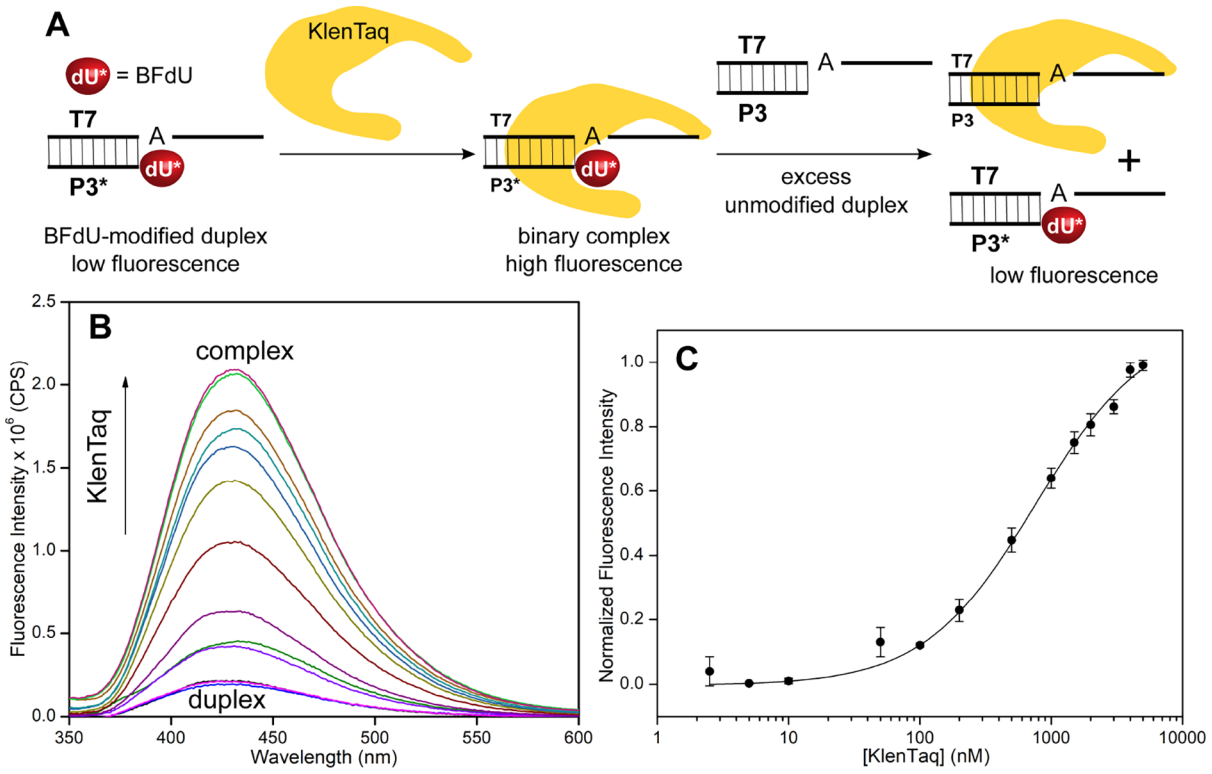


**Figure 5.** Fluorescence of BFdU reports the formation of a binary complex. (A) Scheme for fluorescence monitoring of the binary complex formation and competitive displacement assay. (B) Plot showing the increase in fluorescence intensity of duplex **P3***•**T7** (50 nM) as a function of increasing KlenTaq concentration (0−5 $\mu$M). Samples were excited at 330 nm with excitation and emission slit widths of 7 and 8 nm, respectively. (C) Curve fit for the formation of the binary complex. Normalized fluorescence intensity at $\lambda_{em}$ (430 nm) plotted against concentration of the enzyme.

affinities for the enzyme (Figure S5). Encouraged by these results, we designed an experimental setup to follow the formation of the binary complex by monitoring the changes in the fluorescence of duplex **P3***•**T7** as a function of increasing enzyme concentration (Figure 5A). Here, a BFdU-modified primer sequence (**P3***) the same as **P2*** but without a FAM label was used to avoid the interference from fluorescein. Upon excitation ($\lambda_{max}$ = 330 nm), a concentration-dependent increase in fluorescence intensity with negligible changes in emission maximum ($\lambda_{em}$ = 430 nm) as a result of formation of the binary complex was observed (Figure 5B). A plot of normalized fluorescence intensity *versus* enzyme concentration gave an apparent $K_d$ of 0.76 ± 0.10 $\mu$M, which is comparable to the EMSA data (Figure 5C). BFdU is highly sensitive to micropolarity changes and exhibits enhanced fluorescence intensity and significant red shift in emission maximum when it is located in a polar environment.[59] The free nucleoside analog exhibits a $\lambda_{em}$ of 446 and 423 nm in water and methanol, respectively. When incorporated into ONs, its fluorescence also depends on the neighboring base environment. For example, stacking interaction and electron transfer processes between the modified nucleoside and adjacent bases, particularly with guanine base, lead to fluorescence quenching.[59] On the contrary, rigidification of the fluorophore due to the presence of a molecular rotor element in the probe (benzofuran is attached to the dU ring *via* a rotatable bond) can result in significant enhancement in fluorescence intensity. Therefore, a combination of these factors, in a given nucleic acid conformation, can influence the fluorescence outcome of the probe. The free duplex **P3***•**T7** displays a very low fluorescence intensity due to stacking interaction and free rotation of the fluorophore. In the case of the binary complex, an emission band at 430 nm suggests that BFdU placed in the active site experiences an environment, which is reasonably polar (near methanol). However, the complex exhibits significant enhancement in fluorescence intensity, which is most likely due to the rigidification of the fluorophore in the enzyme pocket.

To prove that the increment in fluorescence intensity is a result of specific binding of the BFdU-labeled DNA duplex in the active site, a competitive displacement binding assay was performed. A binary complex (duplex **P3***•**T7** 50 nM and KlenTaq 1 $\mu$M), which would produce near saturation fluorescence, was prepared and titrated with increasing concentrations of the unlabeled DNA duplex (**P3**•**T7**). Addition of the unlabeled duplex resulted in a progressive decrease in fluorescence intensity due to the displacement of the less emissive modified duplex from the active site (Figure S6). It is to be noted that even a 20-fold excess of the unmodified duplex did not completely displace the modified duplex from the enzyme. We confirmed this competitive displacement process by EMSA also. Much like a binary complex made of the modified duplex, which was hard to displace using unmodified duplex, a complex of the enzyme−unmodified duplex was strong and required an excess of modified duplex to break the complex (Figure S7). Further, addition of enzyme alone to the nucleotide analog did not significantly affect its fluorescence, indicating that the analog does not bind to the free enzyme (Figure S8).


https://doi.org/10.1021/jacs.2c03454
J. Am. Chem. Soc. 2022, 144, 10556−10569

Fluorescence studies using our probe provide further insights on the functioning of the KlenTaq DNA polymerase. The enzyme efficiently incorporated the nucleotide analogs at the 3′-end of the primer, which is consistent with the active site conformation and narrow channel volume observed in the crystal structures (*vide infra*). The enzyme was further able to efficiently extend the singly-labeled primer•template duplex in the presence of native dNTPs to produce the full-length site-specifically labeled product (Figure 4D). For this to happen, the enzyme needs to form a stable binary complex with the 3′-BFdU-labeled primer•template duplex. The competitive fluorescence assay complemented by EMSA indicates that KlenTaq forms a stable complex with the pre-annealed BFdU-labeled duplex (Figure S6).

**Nucleotide Substrate Itself Serves as a Probe to Report Its Incorporation by KlenTaq.** The differences in fluorescence exhibited by the free nucleotide analog BFdUTP **5** and 3′-BFdU-labeled primer•template duplex prompted us to design an assay to detect the activity of KlenTaq (Figure 6A). For this purpose, we used the **P3•T7** primer•template duplex, which would incorporate only one modified nucleotide analog at the 3′-end was used. Addition of BFdUTP to the primer•template duplex or KlenTaq alone produced only a small change in fluorescence intensity (Figure 6B, red and blue curves). Rewardingly, when BFdUTP was added to samples of a binary complex (enzyme and primer•template duplex), each containing increasing concentrations of the enzyme, a significant reduction in fluorescence intensity accompanied by a blue shift in emission maximum (~430 nm) as compared to the free nucleotide analog (dashed black curve, $\lambda_{em}$ = ~445 nm) was observed (Figure 6B). This fluorescence outcome is due to the incorporation of a single BFdUMP at the 3′-end of the primer, which produces a weakly emissive 3′-BFdU-labeled primer•template duplex (**P3*•T7**) as shown in the earlier experiment (see Figure 5B). In a control experiment, a binary complex made of KlenTaq and the **P5•T7** duplex (**P5** contains a ddC at the 3′-end) was added to BFdUTP. Since this primer would not allow the incorporation of the fluorescently modified nucleotide analog, no decrease in fluorescence intensity was observed (magenta curve). Collectively, these results indicate that the nucleotide substrate, which is environment-sensitive, can itself be used as a probe to study the binary complex formation and also the activity of polymerase enzymes, here KlenTaq, by fluorescence spectroscopy.

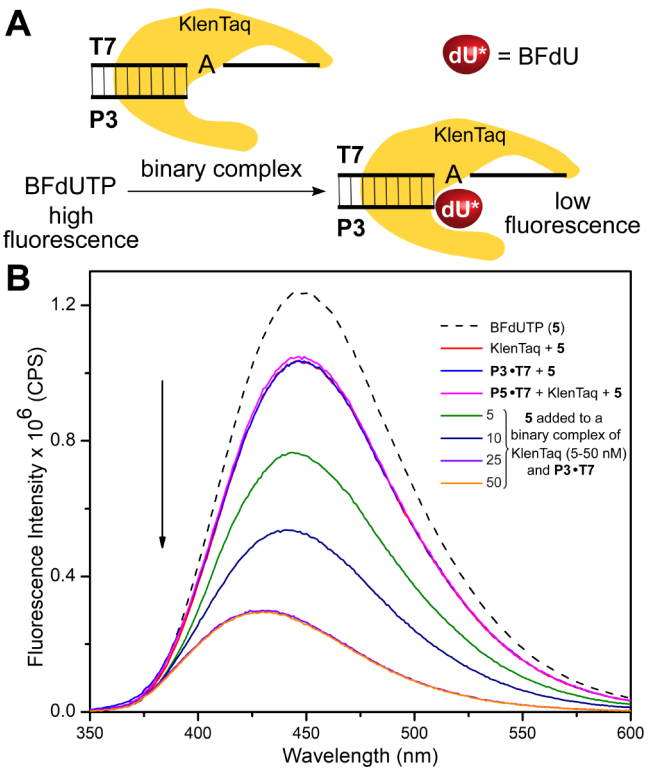


**Figure 6.** BFdU fluorescently reports nucleotide analog incorporation by KlenTaq. (A) Scheme showing the assay setup. (B) Plot showing the decrease in fluorescence intensity of BFdUTP (50 nM) as a function of increasing KlenTaq concentration (0−50 nM) in the presence of the **P3•T7** primer•template duplex (200 nM). Incorporation of BFdUMP at the 3′-end results in a decrease in fluorescence intensity as the labeled duplex shows low fluorescence. In control experiments, addition of KlenTaq (200 nM) or **P3•T7** (200 nM) to BFdUTP (50 nM) showed only small changes in fluorescence intensity. Addition of a binary complex made of 1:1 molar solution (200 nM) of KlenTaq and **P5•T7** duplex (**P5** contains a ddC at the 3′-end) to BFdUTP (50 nM) did not show appreciable reduction in fluorescence intensity. All samples were excited at 330 nm with excitation and emission slit widths of 6 and 7 nm, respectively.

**X-ray Structure of the Ternary Complex Sheds Light on the Incorporation Behavior.** To gain further insights into the incorporation propensities observed in PEX reactions for KlenTaq and KOD DNA polymerases, we planned to solve crystal structures of these enzymes in the replicative state poised to incorporate the fluorescently modified dU*MPs. A template **T8** was designed such that it codes for the incorporation of ddCMP and modified nucleotides as the first and second nucleotides, respectively (Figure 7A). Priming with ddCTP terminates the polymerization process due to the absence of the 3′-OH group, thereby enabling the capture of modified nucleotides in the nucleotide binding site prior to incorporation. Rewardingly, we obtained a high-resolution structure of the ternary closed complex composed of KlenTaq, the primer•template duplex, and BFdUTP (termed KlenTaq-BFdUTP, 1.9 Å, PDB: 7OWF, Figure 7B, Table S4). Crystallization attempts with KOD, however, were unsuccessful. KlenTaq-BFdUTP adopts a structure, which closely resembles the structure of KlenTaq bound to a native nucleoside triphosphate in the nucleotide binding site (PDB: 3RTV, Figure 7B,C).[19] The RMSD value for C$\alpha$ atoms is 0.274 Å (467 atoms aligned). The nucleotide analog is positioned nicely to form complementary Watson−Crick pairing with the templating dA residue in the active site (Figure 7D). The benzofuran and uracil rings are slightly non-coplanar and partially stack with ddCMP incorporated at the 3′-end of the primer (Figure 7D and Figure S9A).

Typical of an active ternary complex, the finger domain is in a closed state and the O helix is placed on top of BFdUTP bound in the active site (Figure 8A). The main difference in KlenTaq-BFdUTP compared to the natural complex is the orientation of the two important amino acid residues Arg660 and Arg587 near the modification (Figure 8A,B). Arg660 usually forms a hydrogen bond to the phosphate backbone of the primer 3′-terminus, which is suggested to stabilize the closed and active conformation in KlenTaq.[81,82] Here, Arg660 flips away from the active site to accommodate the benzofuran modification. Simultaneously, Arg587 moves closer toward the benzofuran ring and is now placed between the benzofuran ring and the phosphate backbone of the 2nd primer nucleotide.


https://doi.org/10.1021/jacs.2c03454
J. Am. Chem. Soc. 2022, 144, 10556−10569

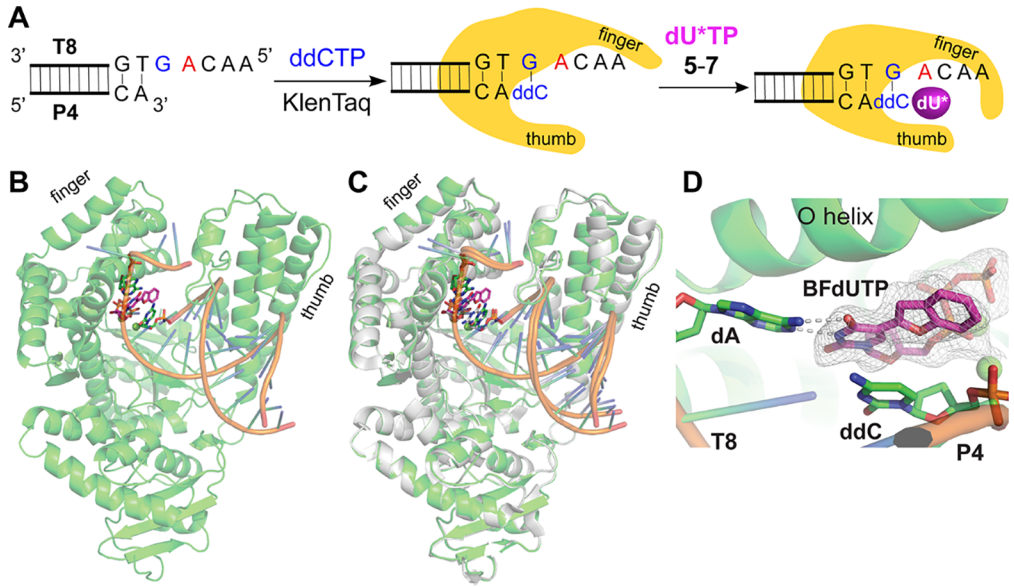


**Figure 7.** (A) Crystallization setup to trap the fluorescent nucleotide probes (**5**–**7**) in the ternary complex. (B) Overall structure of the KlenTaq-BFdUTP ternary complex (green). (C) Superimposition of KlenTaq-BFdUTP (green) with a native KlenTaq ternary complex (gray; PDB: 3RTV). (D) Close-up view of the active site showing the bound nucleotide analog. Depicted is the omit map of BFdUTP at 3$\sigma$. The Watson–Crick base pairing between the nucleotide analog and dA of the template strand is indicated with dashed lines. In all structures, BFdUTP is highlighted in magenta.

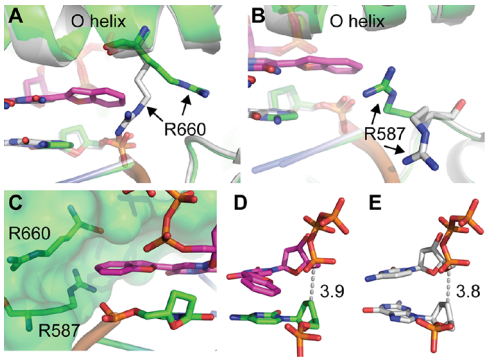


**Figure 8.** (A,B): Superimposition of KlenTaq-BFdUTP (green) and KlenTaq (gray; PDB: 3RTV) highlighting the different orientation of Arg660 and Arg587, respectively. (C) Cleft in which the benzofuran ring is located in the active site is shown. (D,E) Close-up view showing the distance between the $\alpha$-phosphorus and 3′-end of the primer in the ternary complex structures of KlenTaq-BFdUTP and 3RTV, respectively. BFdUTP is highlighted in magenta.

This arrangement results in the formation of a crevice, which nicely encases the heterocycle modification in the nucleotide binding site (Figure 8C and Figure S9B). Relatively high B factors and poor electron density suggest that Arg660 and Arg587 are reasonably flexible. Due to the movement of Arg660, the interaction of the O-helix to the primer backbone is lost, which might contribute to a higher flexibility of the whole finger domain. The distance between the 3′-end carbon atom of the primer and the $\alpha$-phosphorus of the modified nucleotide (3.9 Å) is very similar to the distance observed in the presence of a natural substrate (3.8 Å, for 3RTV), which indicates that the formation of a phosphodiester bond should not be hindered by the presence of the modification (Figure 8D,E). These findings correlate with the efficient incorporation of all three nucleotides in primer extension experiments by KlenTaq. In *Geobacillus stearothermophilus* (Bst) DNA polymerase (another structurally well characterized A family DNA polymerase),[83−85] R703 and R629 residues are analogous to the flexible R660 and R587 residues in KlenTaq.[84] We speculate that Bst could possibly accommodate BFdUTP in the active site in a similar fashion with the help of these two flexible residues and hence could be potentially used to incorporate base-modified nucleotides.

**Structural Data Correlates with KOD and KlenTaq Incorporation and Elongation Behavior.** In general, B family polymerases (e.g., KOD) are more efficient at utilizing base-modified nucleotides compared to the A family polymerases (e.g., KlenTaq).[18,66] A comparative analysis of the structures of ternary complexes of KlenTaq and KOD bound to a native nucleotide or our modified nucleotide analog provides a cogent explanation for the observed differences in the processivity of these families of enzymes (Figure S10).[86] The study identified two main differences between the enzymes to be responsible for the different acceptance of modified substrates (Figure S10A–C). I: The KOD ternary complex exhibits a larger channel within the enzyme[87] that allows diffusion of the triphosphate, leaving of the pyrophosphate as well as accommodation of modifications attached to the nucleobases. II: The DNA conformation close to the active site, which is the B-form in KOD and A-form in the first three primer nucleotides in KlenTaq. B-form DNA is characterized by larger internucleobase distances and a wider major groove compared to A-form DNA offering more space to accommodate major groove modifications as studied here. These two properties could be the reason why KOD (and B-family DNA polymerases in general) is able to incorporate not only one modified nucleotide but also two in a row or one nucleotide apart in more complex template sequences while KlenTaq is unable to incorporate multiple nucleotides with bigger modifications. At the same time, this could explain why KOD (in contrast to KlenTaq) inserts an additional mismatched dU* in the single nucleotide incorporation experiments. An important point considering the elongation


https://doi.org/10.1021/jacs.2c03454
J. Am. Chem. Soc. 2022, 144, 10556−10569

of a modified substrate is the interaction pattern of the protein with the DNA duplex further away from the active site. In KlenTaq as well as in KOD, the primer-template duplex is encased in the groove formed by the thumb and palm domains (Figure 7B,C, Figure S10A).[82] It was shown that the architecture of the tip of the thumb domain making contact with the primer strand differs greatly in the two enzymes (Figure S10D−F).[88] In KOD, the loop formed by residues 668−675 hovers over the minor groove only (Figure S10D), while in KlenTaq, the loop residues 506−509 extend over the phosphate backbone toward the major groove (Figure S10E). This is also the case in the KlenTaq-BFdUTP structure (Figure S10F). A recent structural analysis conducted to probe the movement of C5-ethynylbenzene-modified cytidine along the confines of the KlenTaq enzyme shows the plasticity of the enzyme in accommodating the modification during the course of primer extension.[89] Despite the narrow channel and loop conformation in KlenTaq, primers containing an ethynylbenzene-modified cytidine placed at different positions from the 3′-terminus are well accommodated. Based on this study and the KlenTaq-BFdUTP structure, we infer that the incorporation of a single fluorescent nucleotide analog (irrespective of the heterocycle modification) into the primer does not affect its movement along the channel to produce respective full-length PEX products. However, the narrow channel could potentially attenuate the ability of KlenTaq to insert multiple bulky modifications in close proximity. In support of this notion, SedUTP **7** containing a smaller heterocycle (selenophene) is efficiently processed by KlenTaq to produce full-length products with all the templates, while the enzyme showed poor processivity with the bulkier BFdUTP **5** and BTdUTP **6** substrates, producing truncated products. Taken together, the existing data and present findings provide a cogent understanding on how to choose a polymerase depending on the modification when devising a labeling method. For example, B family polymerases are suited for high density incorporation of fluorescent nucleotide analogs, whereas A family polymerases are more suited for site-specific 3′-end and single internal labeling.

## CONCLUSIONS

A battery of biochemical and structural analyses using responsive fluorescent nucleotide analogs has provided valuable insights into the processing ability of A and B family DNA polymerases. Reactions with different templates that guide the insertion of a single and multiple nucleotide analogs in different phases of the polymerization process indicate differential incorporation behavior of the enzymes, which depends on the size of the heterocycle modification. B family polymerases processed all the nucleotide analogs efficiently to produce ONs with labels at different positions, which was consistent with the situation in the active site (B-form DNA compared to A-from DNA) and the large channel volume available within the enzyme (e.g., KOD) to accommodate the modifications. On the other hand, KlenTaq showed considerable stringency in incorporating bulkier nucleotides particularly at consecutive positions in PEXs. In the single nucleotide incorporation setup, KlenTaq precisely and efficiently added only one modified nucleotide, irrespective of the size of modification in contrast to KOD, which misincorporated a second nucleotide. Therefore, KlenTaq was preferably used in the first step to generate site-specifically labeled ON products. After a purification step, the modified primer can then be fully elongated by further primer extension with either KOD or KlenTaq.

Notably, the BFdU label serves as an efficient fluorescent reporter by providing a real-time read-out for the binary complex formation and enzyme activity under equilibrium conditions. The fluorescence study provides useful insights on the affinity of KlenTaq to bind and process the 3′-end-labeled primer to produce site-specifically labeled ON product. These results expand the utility of our environment-sensitive nucleotide analogs not only as probes for nucleic acid conformational analysis but also as probes for monitoring events in the polymerization process. Further, comparing the native and KlenTaq-BFdUTP structures, the following understanding on the processivity of the polymerase was gained. Three important features of the ternary complex, namely, (i) the flexibility of residues Arg660 and Arg587 near the active site, (ii) the narrow channel within the enzyme, and (iii) the geometry of the primer•template duplex near the active site, appear to be important factors in the processing of heterocycle-modified nucleotides by KlenTaq in this regard. The flexible Arg660 and Arg587 residues serving as "gatekeepers" adopt an altered conformation to accommodate the analogs in the nucleotide binding site, in a manner that allows catalysis to occur. Once the modification is incorporated, the efficiency of the elongation process is now controlled by the plasticity of the channel and the loop that hovers over the major groove side of the primer. In our case, we observe that a smaller modification (SedU) is processed unhamperedly, whereas judicious template design is required for incorporating larger modifications (BFdU and BTdU). Taken together, these new findings will be highly valuable in designing DNA polymerase-compatible nucleotide probes and also in choosing the right enzyme for a given application, namely, site-specific *versus* high density labeling. In the future, we plan to use these nucleotide substrates as probes to study the incorporation mechanism of nucleic acid processing enzymes from human pathogens (e.g., viral polymerases) and develop a discovery platform to identify potential binders by competitive fluorescence-based ligand-binding assay described in this work.

## EXPERIMENTAL SECTION

**PEX with Nucleotide Analogs 5−7.** *Reaction Using KlenTaq and KOD DNA Polymerases.* Primer•template duplexes were prepared by annealing 5′-FAM-labeled primer **P1** (50 $\mu$M) and templates **T1**−**T5** (55 $\mu$M) in a reaction buffer (50 mM Tris−HCl, 16 mM $(NH_4)_2SO_4$, 2.5 mM $MgCl_2$, 0.1% (v/v) Tween 20, pH 8.0) at 95 °C for 3 min. The samples were left to come to room temperature and were placed on an ice bath for 30 min. PEXs were performed at 55 °C in a reaction buffer (50 mM Tris−HCl, 16 mM $(NH_4)_2SO_4$, 2.5 mM $MgCl_2$, 0.1%(v/v) Tween 20, pH 8.0) containing 1.50 $\mu$M of primer•template duplex, 150 $\mu$M of dATP, dGTP, dCTP, dTTP or modified dU*TP (**5**−**7**), and 3 nM KlenTaq/KOD DNA polymerase in a 20 $\mu$L reaction volume. After 45 min, the reaction was quenched by adding 140 $\mu$L of denaturing loading buffer (8.3 M urea in 10 mM Tris−HCl, 100 mM EDTA, 0.05% bromophenol blue, pH 8). The samples were heated at 95 °C for 5 min and then cooled on an ice bath. 5 $\mu$L (0.94 pmol) of the sample was loaded on an analytical 18% denaturing polyacrylamide gel and was electrophoresed at 30 W for 2.5 h. The gel was imaged using a Typhoon gel scanner at a FAM wavelength. Control reactions to study misincorporation were performed in the presence of the primer•template duplex, enzyme, dATP, dGTP, and dCTP but without dTTP or modified dU*TPs.

*Reaction Using Vent(exo-) DNA Polymerase.* A reaction mixture containing 2 $\mu$M primer **P1** and 2.5 $\mu$M templates **T1**−**T5**, 300 $\mu$M of


https://doi.org/10.1021/jacs.2c03454
J. Am. Chem. Soc. 2022, 144, 10556−10569

dATP, dGTP, dCTP, dTTP, or modified dU*TP (**5**−**7**), 1 U/μL of Vent(exo-) in 1× Thermopol reaction buffer (20 mM Tris−HCl, 10 mM $(NH_4)_2SO_4$, 10 mM KCl, 2 mM $MgSO_4$, 0.1% Triton X-100, pH 8.8) was incubated at 60 °C. After 40 min, 180 μL of denaturing loading buffer (8.3 M urea in 10 mM Tris−HCl, 100 mM EDTA, 0.05% bromophenol blue, pH 8) was added to the reaction mix. The samples were heated at 95 °C for 5 min and cooled on an ice bath. 5 μL of the sample (1 pmol) was loaded on an analytical 18% denaturing polyacrylamide gel and was electrophoresed at 30 W for 2.5 h. The gel was imaged using a Typhoon gel scanner at a FAM wavelength. Control reactions to study misincorporation were performed in the presence of the primer•template duplex, enzyme, dATP, dGTP, and dCTP but without dTTP or modified dU*TPs.

*Single Nucleotide Incorporation Assay.* 5′-FAM-labeled primer **P2** (50 μM) and template **T6** (55 μM) were annealed in a reaction buffer (50 mM Tris−HCl, 16 mM $(NH_4)_2SO_4$, 2.5 mM $MgCl_2$, 0.1% (v/v) Tween 20, pH 8.0) at 95 °C for 3 min. The sample was cooled to room temperature and kept on an ice bath for 30 min. Reactions were carried out at 55 °C in a reaction buffer (50 mM Tris−HCl, 16 mM $(NH_4)_2SO_4$, 2.5 mM $MgCl_2$, 0.1% (v/v) Tween 20, pH 8.0) containing 1.5 μM of the annealed primer•template duplex, 150 μM of dTTP or modified dU*TP (**5**−**7**), and 3 nM KlenTaq/KOD DNA polymerase in a 20 μL reaction volume. Reaction aliquots (10 μL) after 15 and 45 min were mixed with 35 μL of denaturing loading buffer (8.3 M urea in 10 mM Tris−HCl, 100 mM EDTA, 0.05% bromophenol blue, pH 8) and heated at 95 °C for 5 min and cooled on an ice bath. 5 μL (1.6 pmol) of the sample was loaded on an analytical 20% denaturing polyacrylamide gel and electrophoresed at 30 W for 2.5 h and imaged using a Typhoon gel scanner at a FAM wavelength.

*Large-Scale Single Nucleotide Incorporation of BFdUTP 5 Using KlenTaq DNA Polymerase.* Single nucleotide incorporation reaction was performed in 840 μL reaction volume using 150 μM BFdUTP **5**, 1.50 μM annealed primer•template duplex (**P2•T6** or **P3•T6**), and 3 nM KlenTaq in 50 mM Tris−HCl buffer (pH 8.0, 16 mM $(NH_4)_2SO_4$, 2.5 mM $MgCl_2$, 0.1% (v/v) Tween 20). The reaction solution was incubated at 55 °C for 45 min. The reaction was heated at 95 °C for 5 min and cooled on an ice bath. The solution was completely concentrated using a SpeedVac, and 300 μL of 5 M ammonium acetate and 700 μL of 100% ethanol were added. The sample was kept at −40 °C for 12 h. The sample was centrifuged at 4 °C at 5000 rpm for 30 min. DNA pellets were collected and washed 3 times with 100% ethanol and dried at room temperature. Nine such reactions were performed using primers **P2** and **P3** to produce BFdU-modified ON **P2*** and **P3***. DNA pellets were pooled together and dissolved in 30 μL of denaturing loading buffer (8.3 M urea in 10 mM Tris−HCl, 100 mM EDTA, 0.05% bromophenol blue, pH 8) and loaded onto a preparative 20% polyacrylamide gel and electrophoresed under denaturing conditions. The gel was UV shadowed, and bands corresponding to the products were excised. The ON products were extracted from the gel using 0.5 M ammonium acetate followed by desalting using a Sep-Pak C18 cartridge. Under these conditions, approximately 70% pure **P2*** and **P3*** was isolated. The mass of ONs was confirmed by ESI mass analysis in negative mode by direct injection of 200 pmol of DNA ONs in 50% ACN (LCMS grade) in 10 mM triethylamine and 100 mM hexafluoro-2-propanol (Table S2 and Figure S4).

*Template-Dependent Site-Specific Labeling.* In a 1.5 mL Eppendorf tube, 150 μM BFdUTP **5** and 1.50 μM annealed primer•template duplex (**P2•T6**) in 50 mM Tris−HCl (pH 8.0), 16 mM $(NH_4)_2SO_4$, 2.5 mM $MgCl_2$, and 0.1% (v/v) Tween 20 were incubated with 3 nM KlenTaq DNA polymerase at 55 °C for 45 min. The total reaction volume was 840 μL (containing 1.26 nmol of primer•template). The reaction was heated at 95 °C for 5 min and cooled on an ice bath. The solution was concentrated nearly to dryness using a SpeedVac, and 300 μL of 5 M ammonium acetate and 700 μL of 100% ethanol were added. The sample was kept at −40 °C for 12 h and was centrifuged at 4 °C at 5000 rpm for 30 min. The pellet was washed 3 times with 100% ethanol to remove the unreacted nucleotide analog and dried at room temperature. The pellet was re-dissolved in 663.6 μL of reaction buffer (50 mM Tris−HCl, 16 mM $(NH_4)_2SO_4$, 2.5 mM $MgCl_2$, 0.1% (v/v) Tween 20, pH 8.0) and annealed at 95 °C for 3 min. The reaction mixture was cooled to room temperature and kept on an ice bath for 30 min. To the same reaction tube, 126 μL of 1 mM dNTPs (dATP, dGTP, dCTP, dTTP) and 50.4 μL 50 nM KOD/KlenTaq DNA polymerase were added and incubated at 55 °C for 45 min. The final concentration of dNTPs was 150 μM and that for enzyme was 3 nM. The reaction was heated at 95 °C for 5 min and cooled on an ice bath. In order to monitor the progress of the reaction, after each step, 10 μL of the reaction mixture was taken and mixed with 35 μL of denaturing loading buffer (8.3 M urea in 10 mM Tris−HCl, 100 mM EDTA, 0.05% bromophenol blue, pH 8). 5 μL samples were loaded onto a sequencing 15% denaturing polyacrylamide gel and electrophoresed at 30 W for 2.5 h. The gel was imaged using Typhoon gel scanner at FAM wavelength.

The remaining solution was concentrated using a SpeedVac, and 300 μL of 5 M ammonium acetate and 700 μL of 100% ethanol were added. The sample was kept at −40 °C for 12 h and was centrifuged at 4 °C at 5000 rpm for 30 min. DNA pellets were collected and washed 3 times with 100% ethanol and dried at room temperature. Four such reactions were performed, and combined DNA pellets were dissolved in 30 μL of denaturing loading buffer (8.3 M urea in 10 mM Tris−HCl, 100 mM EDTA, 0.05% bromophenol blue, pH 8), loaded onto a preparative 15% polyacrylamide gel, and electrophoresed under denaturing conditions. The gel was UV shadowed, and the band corresponding to the full length product was excised. The ON product was extracted from the gel using 0.5 M ammonium acetate followed by desalting using a Sep-Pak C18 cartridge. The identity of the labeled product was confirmed by ESI mass analysis (Figure S4 and Table S2).

*Fluorescence Binding Assay to Determine Binary Complex Formation.* BFdU-modified ON **P3*** (10 μM) was annealed to a template **T7** (10.5 μM) at 95 °C for 3 min in a binding buffer (10 mM Tris−HCl, 50 mM KCl, 5 mM $MgCl_2$, pH 7.9). The stock solution was cooled to room temperature and kept on an ice bath for 30 min. A series of primer•template duplex (**P3*•T7**, 50 nM) samples containing increasing concentrations of KlenTaq (0−5 μM) in the binding buffer were incubated at 25 °C for 45 min. The total volume of each sample was 200 μL. The fluorescence spectrum of individual samples was recorded at 25 °C by exciting the samples at 330 nm with excitation and emission slit widths of 7 and 8 nm, respectively. The amount of glycerol in samples was low (0−1.5%), which should not affect the fluorescence of the BFdU probe. Beyond 1.5% glycerol in the sample results in a slight increase in fluorescence intensity of the duplex itself, possibly due to rigidification of the probe in a more viscous medium (data not shown). The blank spectrum of a sample without the BFdU-modified primer•template duplex (**P3*•T7**) was subtracted from each spectrum. Fluorescence experiments were performed in triplicate. Increasing fluorescence intensity at emission maximum (430 nm) was fit to the Hill equation (Origin 8.5) by plotting normalized fluorescence intensity ($F_N$) versus KlenTaq concentration. A Hill coefficient ($n$) of nearly 1 was observed for binding of the BFdU-labeled primer•template duplex (**P3*•T7**) to KlenTaq DNA polymerase. $R^2$ was close to unity.[17,59]

$$F_N = \frac{F_i - F_0}{F_S - F_0}$$

$F_i$ is the fluorescence intensity measured at each protein concentration. $F_0$ and $F_S$ are the fluorescence intensity measured in the absence of protein and at saturation point. $n$ is the Hill coefficient measuring the degree of cooperativity in binding. $K_d$ is the apparent dissociation constant.

$$F_N = F_0 + (F_S - F_0)\left(\frac{[\text{KlenTaq}]^n}{[K_d]^n + [\text{KlenTaq}]^n}\right)$$

*Fluorescence Detection of Incorporation of the Nucleotide Analog by KlenTaq.* Primer **P3** (10 μM) or 3′-ddCMP-modified primer **P5** (10 μM) was annealed to a template **T7** (10.5 μM) at 95 °C for 3 min in a buffer (10 mM Tris−HCl, 50 mM KCl, 5 mM


https://doi.org/10.1021/jacs.2c03454
J. Am. Chem. Soc. 2022, 144, 10556−10569

$MgCl_2$, pH 7.9). The solution was cooled to room temperature and kept on an ice bath for 30 min. A series of primer-template duplex (**P3•T7**, 200 nM) samples containing increasing concentrations of KlenTaq (0−200 nM) in the above buffer were incubated at 25 °C for 45 min. To each sample, 5 μL of BFdUTP **5** (final conc. 50 nM) was added and incubated at 55 °C for 15 min. The total volume was maintained at 200 μL and glycerol, concentration was less than 0.05%. Samples were cooled to 25 °C and fluorescence was measured at 25 °C. As a control experiment, the **P5•T7** duplex (200 nM) was incubated with KlenTaq (200 nM) at 25 °C for 45 min and BFdUTP (final conc. of 50 nM) was added and kept at 55 °C for 15 min. Another control experiment was performed using the same procedure with sample containing only KlenTaq (200 nM) or the primer•-template duplex. All samples were excited at 330 nm with excitation and emission slit widths of 6 and 7 nm, respectively. Measurements were performed in triplicate.

*Crystallization, Data Collection, and Refinement.* The crystallization trials to obtain the ternary complex of KlenTaq with primer•template duplex and modified dNTPs were set-up as illustrated in Figure 5A. A 1:1 solution of primer **P4** and template **T8** (3 mM) was annealed at 95 °C for 5 min and slowly cooled to 4 °C over 30 min. The sample was diluted with a storage buffer (20 mM Tris−HCl pH 7.5, 1 mM EDTA, 1 mM β-mercaptoethanol, 150 mM NaCl), and a 1:1 solution (1 M) of $MgCl_2$ and $MnCl_2$, KlenTaq (20.9 mg/mL), and ddCTP (10 mM) were added. The reaction solution was incubated at 55 °C for 45 min, after which the modified nucleotide (e.g., BFdUTP, 10 mM) was added and was further incubated at 30 °C for 45 min. The final concentrations of KlenTaq, primer•template duplex, ddCTP, and modified nucleotide were 6.3 mg/mL, 0.12 mM, 0.31 mM and 1.03 mM, respectively (molar ratio 1:1.2:3:10). The final concentration of $MgCl_2$ in the above sample was 20 mM. The sample was filtered using a 0.1 μM sterile filter, and crystals were grown by hanging drop vapor diffusion method by mixing with the reservoir solution (commercial screens) in different ratios. Diffraction-quality crystals with BFdUTP were obtained in a drop composed of a 1:2 ratio of protein to reservoir. Reservoir composition was 16% PEG 6000, 0.1 M Tris pH 8.0 and 0.2 M magnesium formate. The crystals were cryoprotected in the reservoir solution containing 20% ethylene glycol and frozen in liquid nitrogen.

Data was collected at the Swiss Light Source (SLS) of the Paul Scherrer Institute (PSI) in Villigen, Switzerland. Data collection and refinement statistics are summarized in Table S4. Data was processed using the XDS package[90] and the XDSGUI graphical interface (https://strucbio.biologie.uni-konstanz.de/xdswiki/index.php/XDSGUI). The structure was solved by rigid body refinement of the native KlenTaq ternary structure (PDB: 3RTV). Structure refinement was done with phenix.[91] Model building was done in Coot[92,93] and model quality was evaluated by the MolProbity[94] web server (http://molprobity.biochem.duke.edu/) and the PDB validation server (https://validate-rcsb-1.wwpdb.org). Figures were created with PyMOL. For superimposition in figures and RMSD value calculation (after outlier rejection), structures were superimposed in PyMOL using the "align" command. The atomic coordinates and structure factors have been deposited on the Protein Data Bank with the PDB code 7OWF.

## ■ ASSOCIATED CONTENT

### Supporting Information

The Supporting Information is available free of charge at https://pubs.acs.org/doi/10.1021/jacs.2c03454.

Synthesis of nucleotide analogs, experimental details, crystal and characterization data, and supporting figures and tables (PDF)

## ■ AUTHOR INFORMATION


### Corresponding Authors

**Andreas Marx** − *Department of Chemistry and Konstanz Research School Chemical Biology, University of Konstanz, 78457 Konstanz, Germany;* orcid.org/0000-0002-6471-3689; Email: andreas.marx@uni-konstanz.de

**Seergazhi G. Srivatsan** − *Department of Chemistry, Indian Institute of Science Education and Research (IISER), Pune 411008, India;* orcid.org/0000-0001-5765-3967; Email: srivatsan@iiserpune.ac.in

### Authors

**Pulak Ghosh** − *Department of Chemistry, Indian Institute of Science Education and Research (IISER), Pune 411008, India*

**Heike M. Kropp** − *Department of Chemistry and Konstanz Research School Chemical Biology, University of Konstanz, 78457 Konstanz, Germany*

**Karin Betz** − *Department of Chemistry and Konstanz Research School Chemical Biology, University of Konstanz, 78457 Konstanz, Germany*

**Samra Ludmann** − *Department of Chemistry and Konstanz Research School Chemical Biology, University of Konstanz, 78457 Konstanz, Germany*

**Kay Diederichs** − *Department of Biology and Konstanz Research School Chemical Biology, University of Konstanz, 78457 Konstanz, Germany*

Complete contact information is available at: https://pubs.acs.org/10.1021/jacs.2c03454


### Notes

The authors declare no competing financial interest.

## ■ ACKNOWLEDGMENTS

P.G. is thankful to IISER Pune for the graduate research fellowship. We thank Rupam Bhattacharjee for his help in the mass analysis of ONs. P.G. is thankful to the Asian Chemical Biology Initiative (ACBI) Co-Mentorship Program and Professor Motonari Uesugi for valuable discussion. We also acknowledge access to and assistance at the beamlines PXI and PXIII of the SLS at the Paul Scherrer Institute in Villigen (CH). S.G.S. greatly appreciates Alexander von Humboldt-Foundation for a renewed research fellowship constituted for alumni. This work was supported by Wellcome Trust-DBT India Alliance senior fellowship (IA/S/16/1/502360) to S.G.S.

## ■ REFERENCES


(1) Kranaster, R.; Marx, A. Engineered DNA polymerases in biotechnology. *ChemBioChem* **2010**, *11*, 2077−2084.

(2) Chen, T.; Hongdilokkul, N.; Liu, Z.; Thirunavukarasu, D.; Romesberg, F. E. The expanding world of DNA and RNA. *Curr. Opin. Chem. Biol.* **2016**, *34*, 80−87.

(3) Hocek, M. Enzymatic synthesis of base-functionalized nucleic acids for sensing, cross-linking, and modulation of protein−DNA binding and transcription. *Acc. Chem. Res.* **2019**, *52*, 1730−1737.

(4) Klöcker, N.; Weissenboeck, F. P.; Rentmeister, A. Covalent labeling of nucleic acids. *Chem. Soc. Rev.* **2020**, *49*, 8749−8773.

(5) McKenzie, L. K.; El-Khoury, R.; Thorpe, J. D.; Damha, M. J.; Hollenstein, M. Recent progress in non-native nucleic acid modifications. *Chem. Soc. Rev.* **2021**, *50*, 5126−5164.

(6) Jäger, S.; Rasched, G.; Kornreich-Leshem, H.; Engeser, M.; Thum, O.; Famulok, M. A versatile toolbox for variable DNA functionalization at high density. *J. Am. Chem. Soc.* **2005**, *127*, 15071−15082.

(7) Burley, G. A.; Gierlich, J.; Mofid, M. R.; Nir, H.; Tal, S.; Eichen, Y.; Carell, T. Directed DNA metallization. *J. Am. Chem. Soc.* **2006**, *128*, 1398−1399.

(8) Srivatsan, S. G.; Tor, Y. Fluorescent pyrimidine ribonucleotide: synthesis, enzymatic incorporation, and utilization. *J. Am. Chem. Soc.* **2007**, *129*, 2044−2053.
(9) Bentley, D. R.; Balasubramanian, S.; Swerdlow, H. P.; Smith, G. P.; Milton, J.; Brown, C. G.; Hall, K. P.; Evers, D. J.; Barnes, C. L.; Bignell, H. R.; et al. Accurate whole human genome sequencing using reversible terminator chemistry. *Nature* **2008**, *456*, 53−59.
(10) Chen, F.; Gaucher, E. A.; Leal, N. A.; Hutter, D.; Havemann, S. A.; Govindarajan, S.; Ortlund, E. A.; Benner, S. A. Reconstructed evolutionary adaptive paths give polymerases accepting reversible terminators for sequencing and SNP detection. *Proc. Natl. Acad. Sci. U. S. A.* **2010**, *107*, 1948−1953.
(11) Ramsay, N.; Jemth, A.-S.; Brown, A.; Crampton, N.; Dear, P.; Holliger, P. CyDNA: synthesis and replication of highly Cy-dye substituted DNA by an evolved polymerase. *J. Am. Chem. Soc.* **2010**, *132*, 5096−5104.
(12) Winz, M. L.; Linder, E. C.; André, T.; Becker, J.; Jäschke, A. Nucleotidyl transferase assisted DNA labeling with different click chemistries. *Nucleic Acids Res.* **2015**, *43*, No. e110.
(13) Matyašovský, J.; Perlíková, P.; Malnuit, V.; Pohl, R.; Hocek, M. 2-Substituted dATP derivatives as building blocks for polymerase-catalyzed synthesis of DNA modified in the minor groove. *Angew. Chem., Int. Ed.* **2016**, *55*, 15856−15859.
(14) Muttach, F.; Rentmeister, A. A biocatalytic cascade for versatile one-pot modification of mRNA starting from methionine analogues. *Angew. Chem., Int. Ed.* **2016**, *55*, 1917−1920.
(15) Zhou, C. Y.; Alexander, S. C.; Devaraj, N. K. Fluorescent turn-on probes for wash-free mRNA imaging via covalent site-specific enzymatic labeling. *Chem. Sci.* **2017**, *8*, 7169−7173.
(16) Sarac, I.; Hollenstein, M. Terminal deoxynucleotidyl transferase in the synthesis and modification of nucleic acids. *ChemBioChem* **2019**, *20*, 860−871.
(17) George, J. T.; Srivatsan, S. G. Responsive fluorescent nucleotides serve as efficient substrates to probe terminal uridylyl transferase. *Chem. Commun.* **2020**, *56*, 12319−12322.
(18) Hottin, A.; Marx, A. Structural insights into the processing of nucleobase-modified nucleotides by DNA polymerases. *Acc. Chem. Res.* **2016**, *49*, 418−427.
(19) Betz, K.; Malyshev, D. A.; Lavergne, T.; Welte, W.; Diederichs, K.; Dwyer, T. J.; Ordoukhanian, P.; Romesberg, F. E.; Marx, A. KlenTaq polymerase replicates unnatural base pairs by inducing a Watson-Crick geometry. *Nat. Chem. Biol.* **2012**, *8*, 612−614.
(20) Ju, J.; Kim, D. H.; Bi, L.; Meng, Q.; Bai, X.; Li, Z.; Li, X.; Marma, M. S.; Shi, S.; Wu, J.; Edwards, J. R.; Romu, A.; Turro, N. J. Four-color DNA sequencing by synthesis using cleavable fluorescent nucleotide reversible terminators. *Proc. Natl. Acad. Sci. U. S. A.* **2006**, *103*, 19635−19640.
(21) Obeid, S.; Yulikov, M.; Jeschke, G.; Marx, A. Enzymatic synthesis of multiple spin-labeled DNA. *Angew. Chem., Int. Ed.* **2008**, *47*, 6782−6785.
(22) Jarchow-Choy, S. K.; Krueger, A. T.; Liu, H.; Gao, J.; Kool, E. T. Fluorescent xDNA nucleotides as efficient substrates for a template-independent polymerase. *Nucleic Acids Res.* **2011**, *39*, 1586−1594.
(23) Riedl, J.; Pohl, R.; Rulíšek, L.; Hocek, M. Synthesis and photophysical properties of biaryl-substituted nucleos(t)ides. Polymerase synthesis of DNA probes bearing solvatochromic and pH-sensitive dual fluorescent and $^{19}$F NMR labels. *J. Org. Chem.* **2012**, *77*, 1026−1044.
(24) McCoy, L. S.; Shin, D.; Tor, Y. Isomorphic emissive GTP surrogate facilitates initiation and elongation of in vitro transcription reactions. *J. Am. Chem. Soc.* **2014**, *136*, 15176−15184.
(25) Dziuba, D.; Jurkiewicz, P.; Cebecauer, M.; Hof, M.; Hocek, M. A rotational BODIPY nucleotide: an environment-sensitive fluorescence-lifetime probe for DNA interactions and applications in live-cell microscopy. *Angew. Chem., Int. Ed.* **2016**, *55*, 174−178.
(26) Manna, S.; Srivatsan, S. G. Synthesis and enzymatic incorporation of a responsive ribonucleoside probe that enables quantitative detection of metallo-base pairs. *Org. Lett.* **2019**, *21*, 4646−4650.
(27) Magriñá, I.; Toldrà, A.; Campàs, M.; Ortiz, M.; Simonova, A.; Katakis, I.; Hocek, M.; O'Sullivan, C. K. Electrochemical genosensor for the direct detection of tailed PCR amplicons incorporating ferrocene labelled dATP. *Biosens. Bioelectron.* **2019**, *134*, 76−82.
(28) Gramlich, P. M. E.; Wirges, C. T.; Manetto, A.; Carell, T. Postsynthetic DNA modification through the copper-catalyzed azide-alkyne cycloaddition reaction. *Angew. Chem., Int. Ed.* **2008**, *47*, 8350−8358.
(29) Samanta, A.; Krause, A.; Jäschke, A. A modified dinucleotide for site-specific RNA-labelling by transcription priming and click chemistry. *Chem. Commun.* **2014**, *50*, 1313−1316.
(30) Someya, T.; Ando, A.; Kimoto, M.; Hirao, I. Site-specific labeling of RNA by combining genetic alphabet expansion transcription and copper-free click chemistry. *Nucleic Acids Res.* **2015**, *43*, 6665−6676.
(31) Reisacher, U.; Ploschik, D.; Rönicke, F.; Cserép, G. B.; Kele, P.; Wagenknecht, H.-A. Copper-free dual labeling of DNA by triazines and cyclopropenes as minimal orthogonal and bioorthogonal functions. *Chem. Sci.* **2019**, *10*, 4032−4037.
(32) George, J. T.; Azhar, M.; Aich, M.; Sinha, D.; Ambi, U. B.; Maiti, S.; Chakraborty, D.; Srivatsan, S. G. Terminal uridylyl transferase mediated site-directed access to clickable chromatin employing CRISPR-dCas9. *J. Am. Chem. Soc.* **2020**, *142*, 13954−13965.
(33) Salic, A.; Mitchison, T. J. A chemical method for fast and sensitive detection of DNA synthesis in vivo. *Proc. Natl. Acad. Sci. U. S. A.* **2008**, *105*, 2415−2420.
(34) Curanovic, D.; Cohen, M.; Singh, I.; Slagle, C. E.; Leslie, C. S.; Jaffrey, S. R. Global profiling of stimulus-induced polyadenylation in cells using a poly(A) trap. *Nat. Chem. Biol.* **2013**, *9*, 671−673.
(35) Rieder, U.; Luedtke, N. W. Alkene−tetrazine ligation for imaging cellular DNA. *Angew. Chem., Int. Ed.* **2014**, *53*, 9168−9172.
(36) Sawant, A. A.; Tanpure, A. A.; Mukherjee, P. P.; Athavale, S.; Kelkar, A.; Galande, S.; Srivatsan, S. G. A versatile toolbox for posttranscriptional chemical labeling and imaging of RNA. *Nucleic Acids Res.* **2016**, *44*, No. e16.
(37) Zhang, Y.; Kleiner, R. E. A metabolic engineering approach to incorporate modified pyrimidine nucleosides into cellular RNA. *J. Am. Chem. Soc.* **2019**, *141*, 3347−3351.
(38) Nainar, S.; Cuthbert, B. J.; Lim, N. M.; England, W. E.; Ke, K.; Sophal, K.; Quechol, R.; Mobley, D. L.; Goulding, C. W.; Spitale, R. C. An optimized chemical-genetic method for cell-specific metabolic labeling of RNA. *Nat. Methods* **2020**, *17*, 311−318.
(39) Vyas, R.; Zahurancik, W. J.; Suo, Z. Structural basis for the binding and incorporation of nucleotide analogs with L-stereochemistry by human DNA polymerase λ. *Proc. Natl. Acad. Sci. U. S. A.* **2014**, *111*, E3033−E3042.
(40) Bergen, K.; Steck, A. L.; Strütt, S.; Baccaro, A.; Welte, W.; Diederichs, K.; Marx, A. Structures of *KlenTaq* DNA polymerase caught while incorporating C5-modified pyrimidine and C7-modified 7-deazapurine nucleoside triphosphates. *J. Am. Chem. Soc.* **2012**, *134*, 11840−11843.
(41) Obeid, S.; Bußkamp, H.; Welte, W.; Diederichs, K.; Marx, A. Interactions of non-polar and "Click-able" nucleotides in the confines of a DNA polymerase active site. *Chem. Commun.* **2012**, *48*, 8320−8322.
(42) Obeid, S.; Baccaro, A.; Welte, W.; Diederichs, K.; Marx, A. Structural basis for the synthesis of nucleobase modified DNA by *Thermus aquaticus* DNA polymerase. *Proc. Natl. Acad. Sci. U. S. A.* **2010**, *107*, 21327−21331.
(43) Sinkeldam, R. W.; Greco, N. J.; Tor, Y. Fluorescent analogs of biomolecular building blocks: design, properties, and applications. *Chem. Rev.* **2010**, *110*, 2579−2619.
(44) Wachowius, F.; Höbartner, C. Chemical RNA modifications for studies of RNA structure and dynamics. *ChemBioChem* **2010**, *11*, 469−480.


https://doi.org/10.1021/jacs.2c03454
J. Am. Chem. Soc. 2022, 144, 10556−10569

(45) Xu, W.; Chan, K. M.; Kool, E. T. Fluorescent nucleobases as tools for studying DNA and RNA. *Nat. Chem.* **2017**, *9*, 1043−1055.
(46) Benoît, Y. M.; Dziuba, D.; Benhida, R.; Demchenko, A. P.; Burger, A. Probing of nucleic acid structures, dynamics, and interactions with environment-sensitive fluorescent labels. *Front. Chem.* **2020**, *8*, 112.
(47) Sholokh, M.; Sharma, R.; Shin, D.; Das, R.; Zaporozhets, O. A.; Tor, Y.; Mély, Y. Conquering 2-aminopurine's deficiencies: highly emissive isomorphic guanosine surrogate faithfully monitors guanosine conformation and dynamics in DNA. *J. Am. Chem. Soc.* **2015**, *137*, 3185−3188.
(48) Sproviero, M.; Fadock, K. L.; Witham, A. A.; Manderville, R. A. Positional impact of fluorescently modified G-tetrads within polymorphic human telomeric G-quadruplex structures. *ACS Chem. Biol.* **2015**, *10*, 1311−1318.
(49) Wranne, M. S.; Füchtbauer, A. F.; Dumat, B.; Bood, M.; El-Sagheer, A. H.; Brown, T.; Gradén, H.; Grøtli, M.; Wilhelmsson, L. M. Toward complete sequence flexibility of nucleic acid base analogue FRET. *J. Am. Chem. Soc.* **2017**, *139*, 9271−9280.
(50) Eubanks, C. S.; Forte, J. E.; Kapral, G. J.; Hargrove, A. E. Small molecule-based pattern recognition to classify RNA structure. *J. Am. Chem. Soc.* **2017**, *139*, 409−416.
(51) Manna, S.; Sarkar, D.; Srivatsan, S. G. A dual-app nucleoside probe provides structural insights into the human telomeric overhang in live cells. *J. Am. Chem. Soc.* **2018**, *140*, 12622−12633.
(52) Karimi, A.; Börner, R.; Mata, G.; Luedtke, N. W. A highly fluorescent nucleobase molecular rotor. *J. Am. Chem. Soc.* **2020**, *142*, 14422−14426.
(53) Tanpure, A. A.; Srivatsan, S. G. A microenvironment-sensitive fluorescent pyrimidine ribonucleoside analogue: synthesis, enzymatic incorporation, and fluorescence detection of a DNA abasic site. *Chem. − Eur. J.* **2011**, *17*, 12820−12827.
(54) Dziuba, D.; Pospíšil, P.; Matyašovský, J.; Brynda, J.; Nachtigallová, D.; Rulíšek, L.; Pohl, R.; Hof, M.; Hocek, M. Solvatochromic fluorene-linked nucleoside and DNA as color-changing fluorescent probes for sensing interactions. *Chem. Sci.* **2016**, *7*, 5775−5785.
(55) Li, Y.; Fin, A.; McCoy, L.; Tor, Y. Polymerase-mediated site-specific incorporation of a synthetic fluorescent isomorphic G surrogate into RNA. *Angew. Chem., Int. Ed.* **2017**, *56*, 1303−1307.
(56) Sandin, P.; Stengel, G.; Ljungdahl, T.; Börjesson, K.; Macao, B.; Wilhelmsson, L. M. Highly efficient incorporation of the fluorescent nucleotide analogs tC and $tC^{O}$ by Klenow fragment. *Nucleic Acids Res.* **2009**, *37*, 3924−3933.
(57) Nuthanakanti, A.; Ahmed, I.; Khatik, S. Y.; Saikrishnan, K.; Srivatsan, S. G. Probing G-quadruplex topologies and recognition concurrently in real time and 3D using a dual-app nucleoside probe. *Nucleic Acids Res.* **2019**, *47*, 6059−6072.
(58) Nuthanakanti, A.; Boerneke, M. A.; Hermann, T.; Srivatsan, S. G. Structure of the ribosomal decoding site RNA containing a selenium-modified responsive fluorescent ribonucleoside probe. *Angew. Chem., Int. Ed.* **2017**, *56*, 2640−2644.
(59) Tanpure, A. A.; Srivatsan, S. G. Conformation-sensitive nucleoside analogues as topology-specific fluorescence turn-on probes for DNA and RNA G-quadruplexes. *Nucleic Acids Res.* **2015**, *43*, No. e149.
(60) Haidekker, M. A.; Theodorakis, E. A. Molecular rotors—fluorescent biosensors for viscosity and flow. *Org. Biomol. Chem.* **2007**, *5*, 1669−1678.
(61) Förster, T.; Hoffmann, G. Die viskositätsabhängigkeit der fluoreszenzquantenausbeuten einiger farbstoffsysteme. *Z. Phys. Chem.* **1971**, *75*, 63−76.
(62) Sinkeldam, R. W.; Wheat, A. J.; Boyaci, H.; Tor, Y. Emissive nucleosides as molecular rotors. *ChemPhysChem* **2011**, *12*, 567−570.
(63) Noé, M. S.; Sinkeldam, R. W.; Tor, Y. Oligodeoxynucleotides containing multiple thiophene-modified isomorphic fluorescent nucleosides. *J. Org. Chem.* **2013**, *78*, 8123−8128.
(64) Sawai, H.; Ozaki-Nakamura, A.; Mine, M.; Ozaki, H. Synthesis of new modified DNAs by hyperthermophilic DNA polymerase: substrate and template specificity of functionalized thymidine analogues bearing an sp3-hybridized carbon at the C5 $\alpha$-position for several DNA polymerases. *Bioconjugate Chem.* **2002**, *13*, 309−316.
(65) Ghadessy, F. J.; Ramsay, N.; Boudsocq, F.; Loakes, D.; Brown, A.; Iwai, S.; Vaisman, A.; Woodgate, R.; Holliger, P. Generic expansion of the substrate spectrum of a DNA polymerase by directed evolution. *Nat. Biotechnol.* **2004**, *22*, 755−759.
(66) Kuwahara, M.; Nagashima, J.; Hasegawa, M.; Tamura, T.; Kitagata, R.; Hanawa, K.; Hososhima, S.; Kasamatsu, T.; Ozaki, H.; Sawai, H. Systematic characterization of 2′-deoxynucleoside-5′-triphosphate analogs as substrates for DNA polymerases by polymerase chain reaction and kinetic studies on enzymatic production of modified DNA. *Nucleic Acids Res.* **2006**, *34*, 5383−5394.
(67) Gierlich, J.; Gutsmiedl, K.; Gramlich, P. M. E.; Schmidt, A.; Burley, G. A.; Carell, T. Synthesis of highly modified DNA by a combination of PCR with alkyne-bearing triphosphates and click chemistry. *Chem. − Eur. J.* **2007**, *13*, 9486−9494.
(68) Brudno, Y.; Liu, D. R. Recent progress toward the templated synthesis and directed evolution of sequence-defined synthetic polymers. *Chem. Biol.* **2009**, *16*, 265−276.
(69) Cherkasov, D.; Biet, T.; Bäuml, E.; Traut, W.; Lohoff, M. New nucleotide analogues with enhanced signal properties. *Bioconjugate Chem.* **2010**, *21*, 122−129.
(70) Hollenstein, M. Synthesis of deoxynucleoside triphosphates that include proline, urea, or sulfonamide groups and their polymerase incorporation into DNA. *Chem. − Eur. J.* **2012**, *18*, 13320−13330.
(71) Goubet, A.; Chardon, A.; Kumar, P.; Sharma, P. K.; Veedu, R. N. Synthesis of DNA oligonucleotides containing C5-ethynylbenzenesulfonamidemodified nucleotides (EBNA) by polymerases towards the construction of base functionalized nucleic acids. *Bioorg. Med. Chem. Lett.* **2013**, *23*, 761−763.
(72) Dutson, C.; Allen, E.; Thompson, M. J.; Hedley, J. H.; Murton, H. E.; Williams, D. M. Synthesis of polyanionic C5-modified 2′-deoxyuridine and 2′-deoxycytidine-5′-triphosphates and their properties as substrates for DNA polymerases. *Molecules* **2021**, *26*, 2250.
(73) Tanpure, A. A.; Srivatsan, S. G. Synthesis and photophysical characterization of a fluorescent nucleoside analogue that signals the presence of an abasic site in RNA. *ChemBioChem* **2012**, *13*, 2392−2399.
(74) Ménová, P.; Cahová, H.; Plucnara, M.; Havran, L.; Fojta, M.; Hocek, M. Polymerase synthesis of oligonucleotides containing a single chemically modified nucleobase for site-specific redox labelling. *Chem. Commun.* **2013**, *49*, 4652−4654.
(75) Takezawa, Y.; Nakama, T.; Shionoya, M. Enzymatic synthesis of Cu(II)-responsive deoxyribozymes through polymerase incorporation of artificial ligand-type nucleotides. *J. Am. Chem. Soc.* **2019**, *141*, 19342−19350.
(76) Kuba, M.; Kraus, T.; Pohl, R.; Hocek, M. Nucleotide-bearing benzylidene-tetrahydroxanthylium near-IR fluorophore for sensing DNA replication, secondary structures and interactions. *Chem. − Eur. J.* **2020**, *26*, 11950−11954.
(77) Flamme, M.; Röthlisberger, P.; Levi-Acobas, F.; Chawla, M.; Oliva, R.; Cavallo, L.; Gasser, G.; Marlière, P.; Herdewijn, P.; Hollenstein, M. Enzymatic formation of an artificial base pair using a modified purine nucleoside triphosphate. *ACS Chem. Biol.* **2020**, *15*, 2872−2884.
(78) Röthlisberger, P.; Levi-Acobas, F.; Leumann, C. J.; Hollenstein, M. Enzymatic synthesis of biphenyl-DNA oligonucleotides. *Bioorg. Med. Chem.* **2020**, *28*, No. 115487.
(79) Nakama, T.; Takezawa, Y.; Sasaki, D.; Shionoya, M. Allosteric regulation of DNAzyme activities through intrastrand transformation induced by Cu(II)-mediated artificial base pairing. *J. Am. Chem. Soc.* **2020**, *142*, 10153−10162.
(80) Le, B. H.; Nguyena, V. T.; Seo, Y. J. Site-specific incorporation of multiple units of functional nucleotides into DNA using a step-wise approach with polymerase and its application to monitoring DNA structural changes. *Chem. Commun.* **2019**, *55*, 2158−2161.

(81) Li, Y.; Kong, Y.; Korolev, S.; Waksman, G. Crystal structures of the Klenow fragment of Thermus aquaticus DNA polymerase I complexed with deoxyribonucleoside triphosphates. *Protein Sci.* **1998**, *7*, 1116−1123.
(82) Li, Y.; Waksman, G. Crystal structures of a ddATP-, ddTTP-, ddCTP, and ddGTP- trapped ternary complex of Klentaq1: insights into nucleotide incorporation and selectivity. *Protein Sci.* **2001**, *10*, 1225−1233.
(83) Jackson, L. N.; Chim, N.; Shi, C.; Chaput, J. C. Crystal structures of a natural DNA polymerase that functions as an XNA reverse transcriptase. *Nucleic Acids Res.* **2019**, *47*, 6973−6983.
(84) Johnson, S. J.; Taylor, J. S.; Beese, L. S. Processive DNA synthesis observed in a polymerase crystal suggests a mechanism for the prevention of frameshift mutations. *Proc. Natl. Acad. Sci. U. S. A.* **2003**, *100*, 3895−3900.
(85) Chim, N.; Meza, R. A.; Trinh, A. M.; Yang, K.; Chaput, J. C. Following replicative DNA synthesis by time resolved X-ray crystallography. *Nat. Commun.* **2021**, *12*, 2641.
(86) Kropp, H. M.; Diederichs, K.; Marx, A. The structure of an archaeal B-family DNA polymerase in complex with a chemically modified nucleotide. *Angew. Chem., Int. Ed.* **2019**, *58*, 5457−5461.
(87) Kropp, H. M.; Betz, K.; Wirth, J.; Diederichs, K.; Marx, A. Crystal structures of ternary complexes of archaeal B-family DNA polymerases. *PLoS One* **2017**, *12*, No. e0188005.
(88) Bergen, K.; Betz, K.; Welte, W.; Diederichs, K.; Marx, A. Structures of KOD and 9°N DNA polymerases complexed with primer template duplex. *ChemBioChem* **2013**, *14*, 1058−1062.
(89) Kropp, H. M.; Dürr, S. L.; Peter, C.; Diederichs, K.; Marx, A. Snapshots of a modified nucleotide moving through the confines of a DNA polymerase. *Proc. Natl. Acad. Sci. U. S. A.* **2018**, *115*, 9992−9997.
(90) Kabsch, W. XDS. *Acta Crystallogr., Sect. D: Biol. Crystallogr.* **2010**, *66*, 125−132.
(91) Adams, P. D.; Afonine, P. V.; Bunkóczi, G.; Chen, V. B.; Davis, I. W.; Echols, N.; Headd, J. J.; Hung, L.; Kapral, G. J.; GrosseKunstleve, R. W.; McCoy, A. J.; Moriarty, N. W.; Oeffner, R.; Read, R. J.; Richardson, D. C.; Richardson, J. S.; Terwilliger, T. C.; Zwart, P. H. PHENIX: a comprehensive Python-based system for macromolecular structure solution. *Acta Crystallogr., Sect. D: Biol. Crystallogr.* **2010**, *66*, 213−221.
(92) Emsley, P.; Cowtan, K. Coot: model-building tools for molecular graphics. *Acta Crystallogr., Sect. D: Biol. Crystallogr.* **2004**, *60*, 2126−2132.
(93) Emsley, P.; Lohkamp, B.; Scottc, W. G.; Cowtan, K. Features and development of *Coot*. *Acta Crystallogr., Sect. D: Biol. Crystallogr.* **2010**, *66*, 486−501.
(94) Chen, V. B.; Arendall, W. B., III; Headd, J. J.; Keedy, D. A.; Immormino, R. M.; Kapral, G. J.; Murray, L. W.; Richardson, J. S.; Richardson, D. C. MolProbity: all-atom structure validation for macromolecular crystallography. *Acta Crystallogr., Sect. D: Biol. Crystallogr.* **2010**, *66*, 12−21.




https://doi.org/10.1021/jacs.2c03454
J. Am. Chem. Soc. 2022, 144, 10556−10569